ISSN: 0067-2904

Plasma Characteristics of the Earth's Ionosphere in F-layer

Aseel A. Temur[2], Ala F. Ahmed[1*]
[1]*Department of Astronomy and Space, College of Science, University of Baghdad, Baghdad, Iraq*
[2]*Department of Radiology and Sonar Techniques, Al- Esraa University College, Baghdad, Iraq*

Received: 18/9/2021 Accepted: 5/11/2021 Published: 30/7/2022

Abstract

In this research, the plasma parameters of the ionospheric F-layer have been calculated during daytime at 12 PM condition for four different months (January ,April, July and October) over Iraqi capital " Baghdad" (44.3^0 E, 33.3^0 N) during the year 2019 that represents the beginning of the solar cycle 25. Depending on the impact of the solar activity that was represented by the number of sunspot (SSN) and solar flux ($F_{10.7}$ cm) on the variation and behavior of the electron density (n_e) and the electron temperature (T_e) which have been conducted using the international reference ionosphere (IRI −2016) model which was considered as one of the recommended international models for different heights (150 − 500) km with 50 km increment. It has been noticed that the seasonal variations of electron density (n_e) and frequency ($\boldsymbol{f}_{pe}$) around the equinoxes are higher than those in summer and winter for solar minimum (2019).While λ_{De} around the equinoxes (April and October) is lower than that of summer and winter for solar minimum (2019). It has been explained as a positive correlation between the thermal velocity of electron (υ_{te}) and (T_e) in all seasonal variation of ionosphere for the selected year. In this paper, the weakness of the electron coupling parameter in the ionosphere was proved in all seasons of the year 2019.

Keywords: Ionosphere; Electron temperature and density, Plasma parameters; SSN; $F_{10.7}$ cm, IRI model; Solar cycle 25.

خصائص البلازما للغلاف الأيوني للأرض في الطبقة F

اسيل عبد تمر[1,2] , الاء فاضل احمد[1*]
[1]قسم الفلك والفضاء, كلية العلوم, جامعة بغداد, بغداد, العراق
[2] قسم تقنيات الاشعة والسونار , كلية الاسراء الجامعة, بغداد, العراق

الخلاصة

في هذا البحث، تم حساب معلمات البلازما لطبقة الأيونوسفير F خلال النهار عند الساعة 12 ظهراً ولمدة أربعة أشهر مختلفة (كانون الثاني ، نيسان ، تموز ، تشرين الأول) فوق العاصمة العراقية "بغداد" (44.3^0 شرقاً ، 33.3^0 شمالاً) خلال عام 2019. العام الذي يمثل بداية الدورة الشمسية 25. اعتمادًا على تأثير النشاط الشمسي الذي يمثله عدد البقع الشمسية (SSN) والتدفق الشمسي ($F_{10.7}$ cm) على تباين وسلوك كثافة الإلكترون (n_e) ودرجة حرارة الإلكترون (T_e) التي تم أخذها باستخدام نموذج الأيونوسفير المرجعي الدولي (IRI −2016) والذي يعتبر أحد النماذج العالمية الموصى بها لارتفاعات مختلفة (150− 500) كم بزيادة قدرها 50 كم. لوحظ أن التغيرات الموسمية لكثافة الإلكترون (n_e) والتردد ($\boldsymbol{f}_{pe}$) حول

*Email: ala.fadil77@gmail.com

الاعتدالات أعلى من تلك في الصيف والشتاء للحد الأدنى للشمس (2019). بينما λ_{De} حول الاعتدال (أبريل و أكتوبر) أقل من الصيف و الشتاء بالنسبة للحد الأدنى من الطاقة الشمسية. تم ايضاح وجود ارتباط إيجابي بين السرعة الحرارية للإلكترون (υ_{te}) و (T_e) في جميع التغيرات الموسمية للغلاف الأيوني للسنة المختارة. في هذا البحث، تم إثبات ضعف معامل اقتران الالكترون في طبقة الايونوسفير في جميع فصول عام 2019.

1. Introduction

The ionosphere is formed in the upper part of the atmosphere by absorbing the incoming solar radiation and creating the ion–electron pairs [1]. In 2011 when O. V. Mingalev, et al., concluded that the temporal evolution of irregularities plasma, having initial cross-section dimension is related directly with a Debye length [2]. S. Sodha and S. K. Mishra (2017) studied the effect of dust insertion in the F-layer ionospheric plasma [3]. Plasma is a quasi – neutral gas consisting of positively and negatively charged particles (usually ions and electrons) and neutral particles which are subject to electric, magnetic and other forces, and which exhibit collective behavior [4-6]. In a strongly ionized medium, the reactions of charged particles due to Coulomb forces predominate. While in a weakly ionized medium, the charged particles interactions and neutral particles predominate [7]. The ionosphere is the part of the Earth upper atmosphere that lies approximately between (50-1000) km above the surface of the Earth [8]. The ionosphere can be divided into three layers called D, E and F layer from low altitude to high altitude. (Figure 1) shows the major ionospheric layers during the day and at night [9]. The region of the ionosphere between the F_2 layer (F_2 layer: 250-500 km) and the upper boundary of the ionosphere is defined as the topside layer of the ionosphere. This research has been conducted to investigate the effect of solar activity on earth ionosphere and calculated plasma characteristics in F layer or the mentioned altitudes [8].

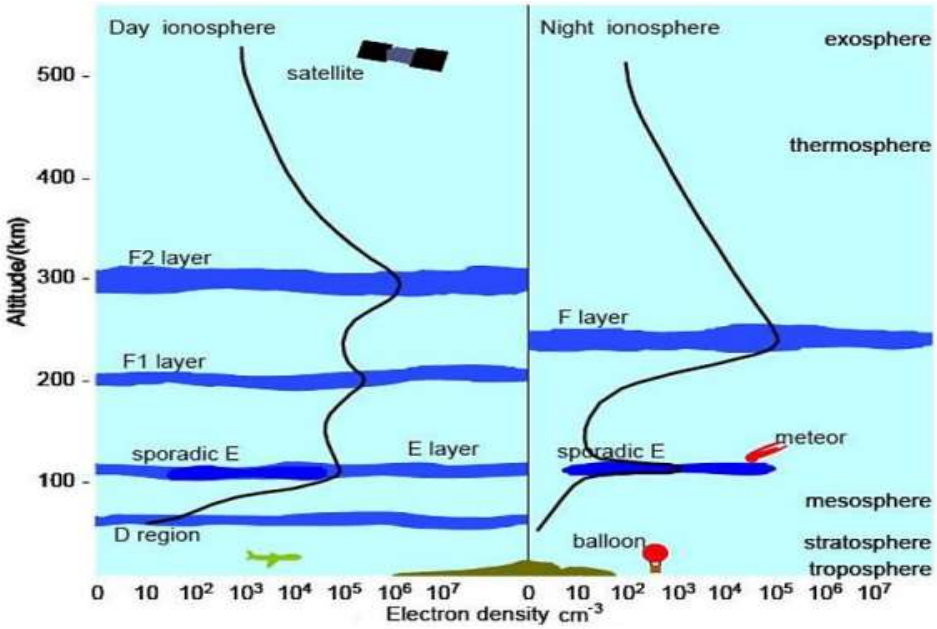

Figure 1- Day and night structure of the ionosphere [9].

From Figure 1, we can see during the nighttime that the ionosphere only has two layers, E layer and F layer. During the daytime, because of the increased ionization by ultraviolet (UV) light and X-ray of the sun, F layer consists of F_1 and F_2 layer (F_1 layer: 150-250 km; F_2 layer: 250-500 km), (E layer: 90-150 km) and a new layer (D layer: 50-90 km) appears below E layer [9].

2. Plasma parameters

A plasma is described by a number of parameters like, its density of electron n_e, temperature T, magnetic field *B*, macroscopic neutrality, plasma frequency of electron ω_{pe}, Debye length λ_D, and the particles number in a Debye sphere N_D [10].

- **Debye length of electron (λ_{De}):** One important feature of the plasma is that it will exhibit group behavior, thus the plasma particles will be controlled by the long-range electromagnetic forces rather than by collisions as is the case in natural gas. The Debye shielding phenomenon is a fundamental property of plasma and gives an example of collective behavior [11].

$$\lambda_{De} = \sqrt{\frac{\varepsilon_\circ k_B T_e}{n_e e^2}} = 69\sqrt{\frac{T_e}{n_e}} \quad (1)$$

Where: T_e in Kelvin, n_e in m^{-3}, K_B is Boltzmann constant (K_B=1.38x10^{-23} JK^{-1}), λ_{De} is Debye length associated to electrons (m), T_e is the temperature of electron, n_e is the density of electron, e is the charge of electron (e =1.602x10^{-19} C), $\varepsilon_\circ$ is the permittivity of free space ($\varepsilon_\circ$= 8.85 × 10^{-12} Fm^{-1}).

- **Plasma frequency of electron (ω_{pe}):** One of the most prominent properties of plasma in the ionosphere is the plasma frequency. The plasma frequency induced by oscillations in the plasma due to electric fields changes daily due to fluctuations in the density of the number of particles [11].

$$\omega_{pe} = \sqrt{\frac{n_e e^2}{\varepsilon_\circ m_e}} \quad (2)$$

Where: m_e is the mass of electron (m_e=9.11x10^{-31}kg).
And in frequency units, given approximately by:

$$f_{pe} = \frac{\omega_{pe}}{2\pi} = 8.98\sqrt{n_e} \quad (3)$$

- **Number of particles in a Debye sphere (N_D):** This parameter associated with the Debye length is the particles number (N_D) in a Debye sphere of radius equal to λ_D. The shielding effect can only occur if the Debye sphere contains a large number of electrons, whose number is given by [12].

$$N_D = \frac{4\pi}{3} n_e \lambda_{De}^3 = 1.38 \times 10^6 \frac{T^{\frac{3}{2}}}{n^{\frac{1}{2}}} \quad (4)$$

According to the above equation, N_D must be much greater than unity to achieve the collective characteristic of plasma $N_D >> 1$ [13].

- **Plasma coupling parameter of electron (Γ):** is the ratio between the minimum distance between two repelling charged particles (r_c) and the average separation between particles (r_d) provided by the density of plasma $r_d \sim n_e^{-1/3}$ [14].

$$r_c = \frac{e^2}{4\pi\epsilon_0 K_B T} \quad (5)$$

$$\Gamma = \frac{r_c}{r_d} = \frac{e^2 n_e^{1/3}}{4\pi\epsilon_0 K_B T} = \frac{1}{4\pi} \times \frac{n_e e^2}{4\pi\epsilon_0 K_B T} \times n_e^{1/3} = \frac{1}{4\pi} \times \frac{n_e e^2}{4\pi\epsilon_0 K_B T} \times n_e^{-2/3} = \frac{1}{4\pi} \times \frac{1}{(n_e \lambda_{De}^3)2/3} \quad (6)$$

It might introduce the number $N_D \sim n_e \lambda_{De}^3$

$$\Gamma \sim \frac{1}{4\pi} \times \frac{1}{(n_e \lambda_{De}^3)2/3} \sim \frac{1}{4\pi} \frac{1}{N_D^{2/3}}$$

$$\Gamma = \frac{1}{(4\pi \lambda_{De}^2 n_e^{2/3})} \quad (7)$$

It can be found that strongly coupled plasmas tend to be cold and dense, such as laser ablation plasma, while weakly coupled plasmas are diffuse and hot and are commonly found in ionosphere and nuclear fusion [15].

- **Thermal velocity of electron (υ_{te}):** The fast time scale of plasma is determined by the frequency ω_{pe} in which the electron obeys to time-dependent fluctuations in the local electric field. We can also explain the timescale related to the frequency of plasma ω_{pe} as proportional

to the time at which the velocity of the thermal electron is given by [10, 14].

$$\upsilon_{te} = \omega_{pe}\, \lambda_{De}$$

$$\upsilon_{te} = \sqrt{\frac{K_B T_e}{m_e}} \tag{8}$$

3. International Reference Ionosphere Model (IRI)

The International Reference Ionosphere (IRI) project was initiated by the Commission for Space Research (COSPAR) and the International Union of Radio Science (URSI) in the late 1960s, (IRI) is the international standard for the features of the density and temperatures of ionosphere [16]. The latest version of IRI contained many important enhancements and new additions. These changes included not only the representation of electron density, but also the electron temperature and ionic composition. The latest version of the IRI-2016 model was selected in this study because this model represented the best model and solution in the ionosphere [17].

4. Results and Discussions

In this work, the selected year of 2019 represents the beginning and minimum of the solar cycle 25. Smoothed Sunspot Number (SSN) and Smoothed Solar Radio Flux ($F_{10.7}$ cm) for the selected year are shown in Table (1).

Table1- Smoothed Sunspot Number (SSN) and Smoothed Solar Radio Flux ($F_{10.7}$ cm) [18].

Month	Jan.	Fab.	Mar.	Apr.	May	Jun.	Jul.	Aug.	Sep.	Oct.	Nov.	Dec.
SSN	5.4	5.0	4.5	4.3	3.9	3.7	3.5	3.4	3.1	2.6	2.0	1.8
$F_{10.7}$	70.0	69.8	69.7	69.6	69.6	69.7	69.7	69.8	69.7	69.5	69.3	69.3

Figure-2 Shows the observed sunspot number for solar cycle 25.

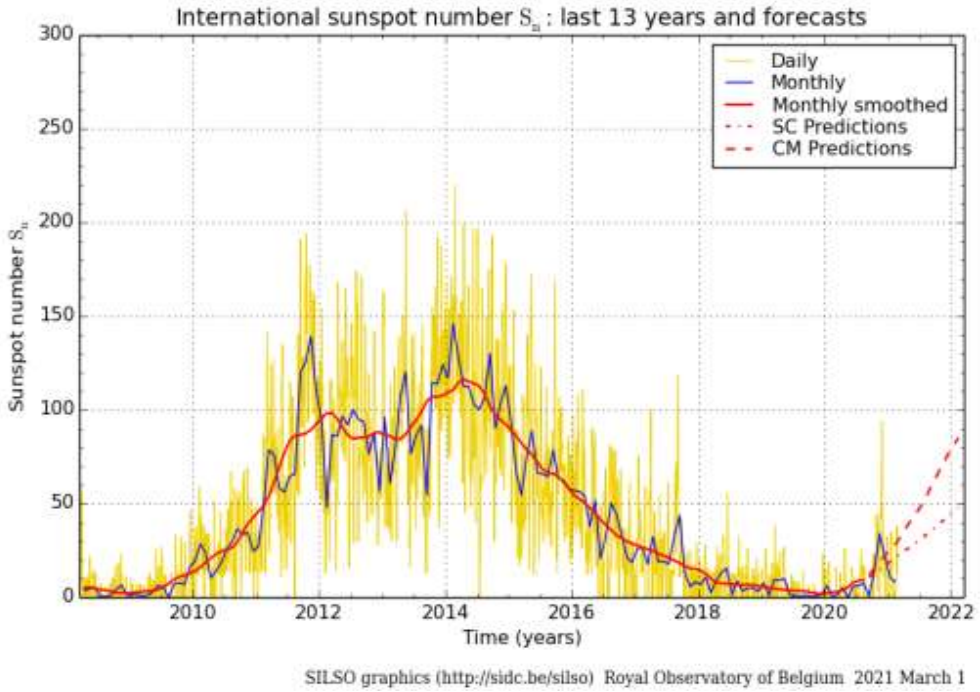

Figure 2-The observed sun spots for the 25 solar cycle [18].

In this research, plasma characteristics were calculated by dividing the studied year into four periods, each period represented the seasonal variations for a specific studied area. For Baghdad station, the seasonal variations were classified according to the following table:

Table 2-Seasonal classification

Seasons	Months		
Winter	December	January	February
Spring	March	April	May
Summer	June	July	August
Autumn	September	October	November

Figures-3 and -4 show the diurnal variation of electron temperature (T_e) and electron density (n_e) of F-ionosphere layer calculated at different altitudes (150 − 500) km with 50 km increment at four different months during local hours of one day. The dataset of (T_e) and (n_e) were obtained from the (IRI −2016) and the outputs from IRI model were prepared using the Microsoft Excel program.

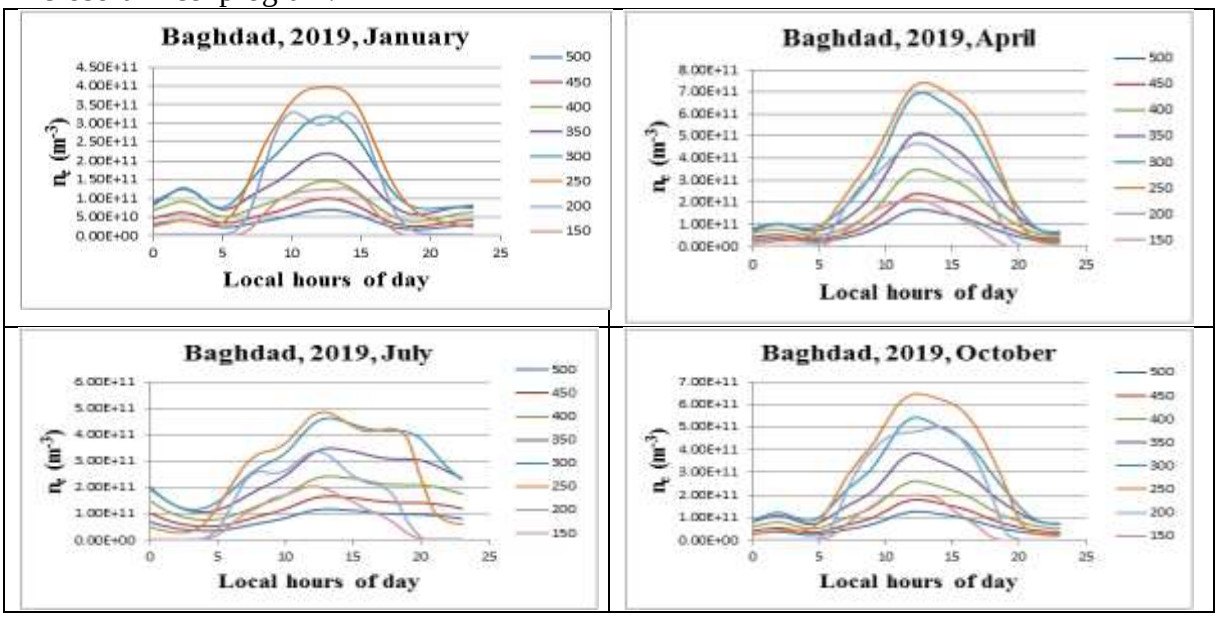

Figure 3- Samples of the diurnal variation of electron temperature (T_e) of F-ionosphere layer calculated at different altitudes (150 − 500) km with 50 km increment in (January, April, July and October) during local hours of one day. Note that T_e increases at 12 PM.

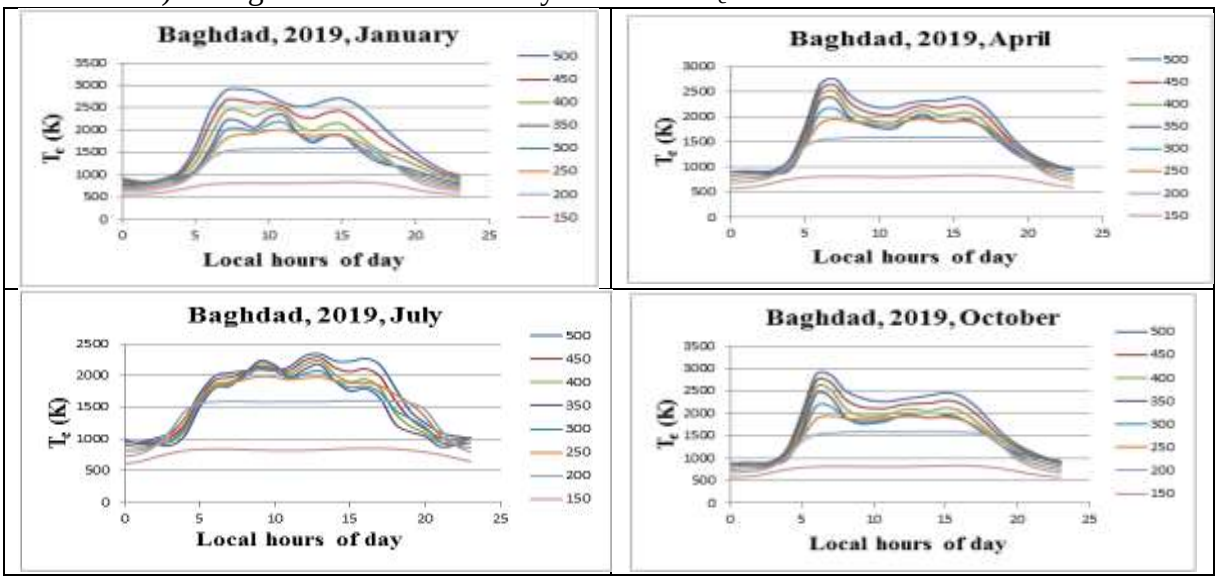

Figure 4-Samples of the diurnal variation of electron density (n_e) of F-ionosphere layer calculated at different altitudes (150 − 500) km with 50 km increment in (January, April, July and October) during local hours of one day. Note that n_e increases at 12 PM.

In this work, the affection of the solar activity for the altitudes (150 – 500) km with 50 km increment on the ionospheric plasma parameters were studied. Figures-3 and -4 show that the values of the density and temperature of electrons were increasing at daytime, hence the ionospheric plasma parameters were calculated at local time 12 PM for the mentioned heights such as λ_{De}, f_{pe}, N_D, Γ and υ_{te} for each altitude.

Table 3-Plasma parameters of F-ionosphere layer calculated at different altitudes (150 – 500) Km with 50 Km increment in January at 12 PM over Iraqi capital "Baghdad" of the year 2019.

Height(km)	T_e(K)	n_e(m^{-3})	λ_{De}(m)	f_{pe}(Hz)	N_D	Γ (m)	υ_{te}(m/s)
150	810.5	1.23E+11	5.60E-03	3.15E+06	9.05E+04	0.000102	110865.22
200	1587.9	2.96E+11	5.05E-03	4.89E+06	1.60E+05	7.018E-05	155178.09
250	1917.9	3.96E+11	4.80E-03	5.65E+06	1.84E+05	6.403E-05	170542.1
300	1909.2	3.18E+11	5.35E-03	5.06E+06	2.03E+05	5.978E-05	170154.9
350	1915.2	2.18E+11	6.47E-03	4.19E+06	2.47E+05	5.255E-05	170422.1
400	2108.1	1.46E+11	8.29E-03	3.43E+06	3.48E+05	4.177E-05	178798.7
450	2316	9.88E+10	1.06E-02	2.82E+06	4.88E+05	3.338E-05	187407.9
500	2523.8	6.94E+10	1.32E-02	2.37E+06	6.62E+05	2.722E-05	195634.8

Table 4-Plasma parameters of F-ionosphere layer calculated at different altitudes (150 - 500) km with 50 km increment in April at 12 PM over Iraqi capital "Baghdad" of the year 2019.

Height(km)	T_e(K)	n_e(m^{-3})	λ_{De}(m)	f_{pe}(Hz)	N_D	Γ (m)	υ_{te}(m/s)
150	808.7	2.12E+11	4.26E-03	4.13E+06	6.87E+04	0.000123	110742.05
200	1587.3	4.64E+11	4.04E-03	6.12E+06	1.28E+05	8.156E-05	155148.7
250	1928.9	7.23E+11	3.56E-03	7.64E+06	1.37E+05	7.781E-05	171030.5
300	1934.9	6.83E+11	3.67E-03	7.42E+06	1.42E+05	7.611E-05	171296.3
350	1947.9	5.05E+11	4.29E-03	6.38E+06	1.66E+05	6.836E-05	171870.8
400	2050.2	3.45E+11	5.32E-03	5.27E+06	2.17E+05	5.72E-05	176326.2
450	2159.7	2.36E+11	6.60E-03	4.36E+06	2.84E+05	4.78E-05	180973.7
500	2269.1	1.65E+11	8.09E-03	3.65E+06	3.66E+05	4.042E-05	185500.7

Table 5-Plasma parameters of F-ionosphere layer calculated at different altitudes (150 – 500) km with 50 km increment in July at 12 PM over Iraqi capital "Baghdad" of the year 2019.

Height(km)	T_e(K)	n_e(m^{-3})	λ_{De}(m)	f_{pe}(Hz)	N_D	Γ (m)	υ_{te}(m/s)
150	820.9	2.05E+11	4.37E-03	4.07E+06	7.14E+04	0.00012	111574.2
200	1587.8	3.35E+11	4.75E-03	5.20E+06	1.50E+05	7.31E-05	155173.2
250	1961	4.73E+11	4.44E-03	6.18E+06	1.74E+05	6.64E-05	172447.7
300	2030.7	4.40E+11	4.69E-03	5.96E+06	1.90E+05	6.26E-05	175485.6
350	2100.1	3.30E+11	5.50E-03	5.16E+06	2.30E+05	5.50E-05	178459.1
400	2169.9	2.30E+11	6.70E-03	4.31E+06	2.90E+05	4.72E-05	181400.5
450	2239.8	1.59E+11	8.19E-03	3.58E+06	3.66E+05	4.04E-05	184299.2
500	2309.7	1.13E+11	9.86E-03	3.02E+06	4.54E+05	3.5003E-05	187152.9

Table 6-Plasma parameters of F-ionosphere layer calculated at different altitudes (150 – 500) km with 50 km increment in October at 12 PM over Iraqi capital "Baghdad" of the year 2019.

Height(km)	T_e(K)	n_e(m^{-3})	λ_{De}(m)	f_{pe}(Hz)	N_D	Γ (m)	υ_{te}(m/s)
150	811.6	1.99E+11	4.41E-03	4.01E+06	7.13E+04	0.000120	110940.4
200	1587.6	4.78E+11	3.98E-03	6.21E+06	1.26E+05	8.235E-05	155163.4
250	1931.5	6.45E+11	3.78E-03	7.21E+06	1.45E+05	7.480E-05	171145.7
300	1944.5	5.41E+11	4.14E-03	6.61E+06	1.60E+05	7.007E-05	171720.7
350	1964.7	3.84E+11	4.94E-03	5.56E+06	1.93E+05	6.186E-05	172610.4
400	2077.9	2.61E+11	6.16E-03	4.59E+06	2.55E+05	5.143E-05	177513.4
450	2198.6	1.79E+11	7.65E-03	3.80E+06	3.35E+05	4.286E-05	182596.2
500	2319.2	1.27E+11	9.32E-03	3.20E+06	4.31E+05	3.624E-05	187537.4

Figure-5 shows the sample of the seasonal variations of electron temperatures (T_e) for eight altitudes (150, 200, 250, 300, 350, 400, 450 and 500) km during low solar activity (2019) over Iraqi capital "Baghdad" region for the adopted model (IRI). This parameter for all months increased with altitudes and reached its maximum at 200 km then it started to be constant until it reached at 400 km and it began to increase with height increment.

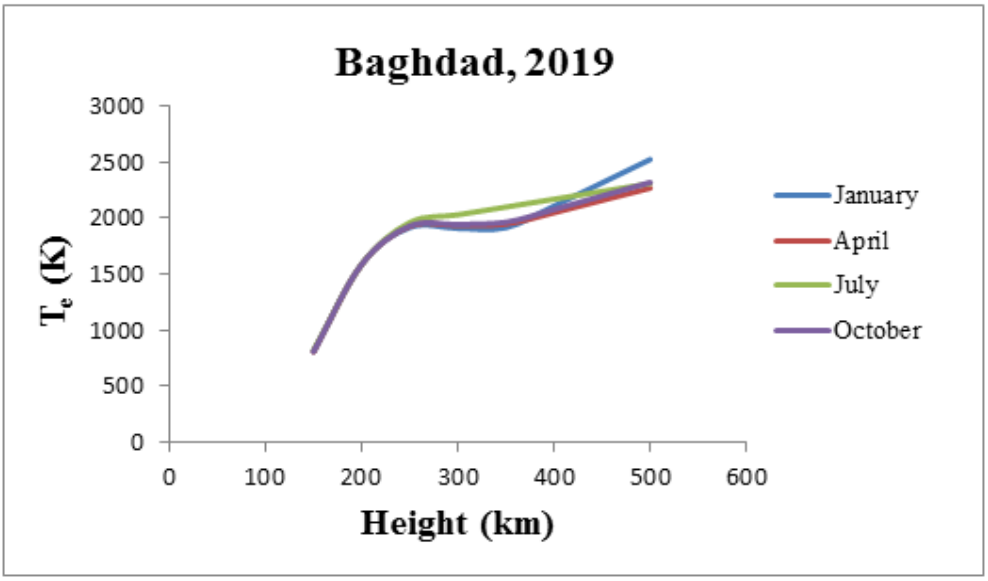

Figure 5-Represented the variation of electron temperature (T_e) at 12 PM of F-ionosphere layer at different altitudes (150 – 500) km with 50 km increment in (January, April, July and October).

Figure-6 shows that the calculations of the n_e parameter varied with increasing the altitude parameter, so it increased with increasing altitude and reached its maximum value at 250 km in all months due to high solar activity that led to the enhancement of solar EUV flux, which increased the photo-ionization production rate that caused the increasing of n_e, then it started to decline with increasing height. The calculations of the n_e parameter showed that their values were higher in April than the months of January, July and October and the values of October were higher than the values of July and April, also the values of July were higher than the values of January.

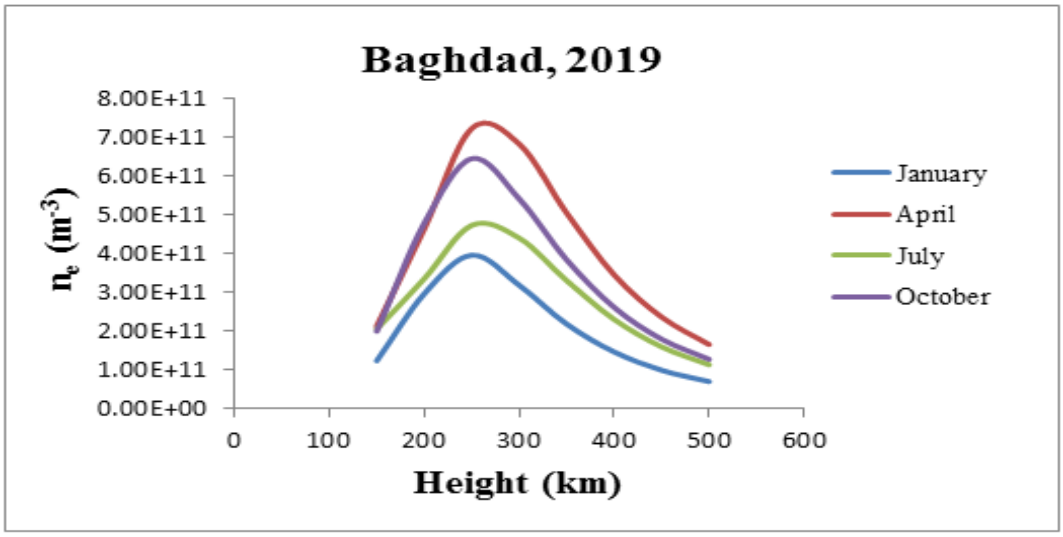

Figure 6-Represented the variation of electron density (n_e) at 12 PM of F-ionosphere layer at different altitudes (150 – 500) km with 50 km increment in (January, April, July and October).

Figure-7 shows that the Debye length of electron, λ_{De} decreased in the altitude range of 200 km - 300 km. This may be due to the increment of the ionization process at this altitude of F-ionosphere layer. Then, it increased with height until it reached its maximum in the altitudes 500 km. However, the rate of recombination exceeded the rate of ionization, and the density of the ionized layers began to decrease. In addition, λ_{De} around the equinoxes (April and October) were less than those in summer or winter for solar minimum (2019). This may be due to the ionization process increasing at equinoxes and which decreased in summer and winter because of the seasonal anomaly.

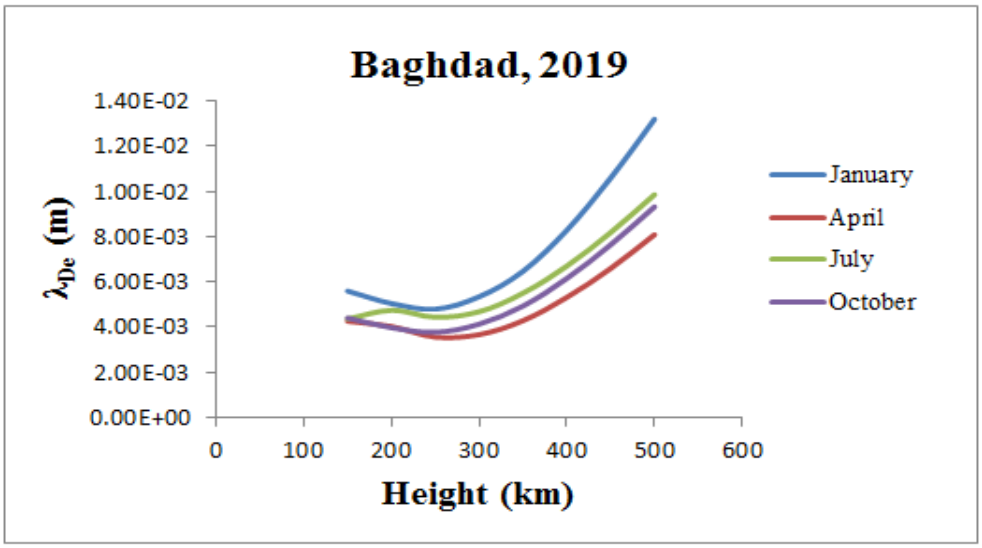

Figure 7-Represented the variation of Debye length of electron, λ_{De} (m) at 12 PM of F-ionosphere layer calculated at different altitudes (150 − 500) km with 50 km increment in (January, April, July and October).

In Figure-8, it is apparent that the Plasma frequency of electron, f_{Pe} increased with height until it reached its maximum in the altitude range of 200 km - 300 km. This may be due to the increment of the ionization process at this altitude of F-ionosphere layer. Then, f_{Pe} began to fall with height when the ionosphere started to merge with the outer space. In addition, frequencies around the equinoxes (April and October) were higher than those in summer or winter for solar minimum (2019).

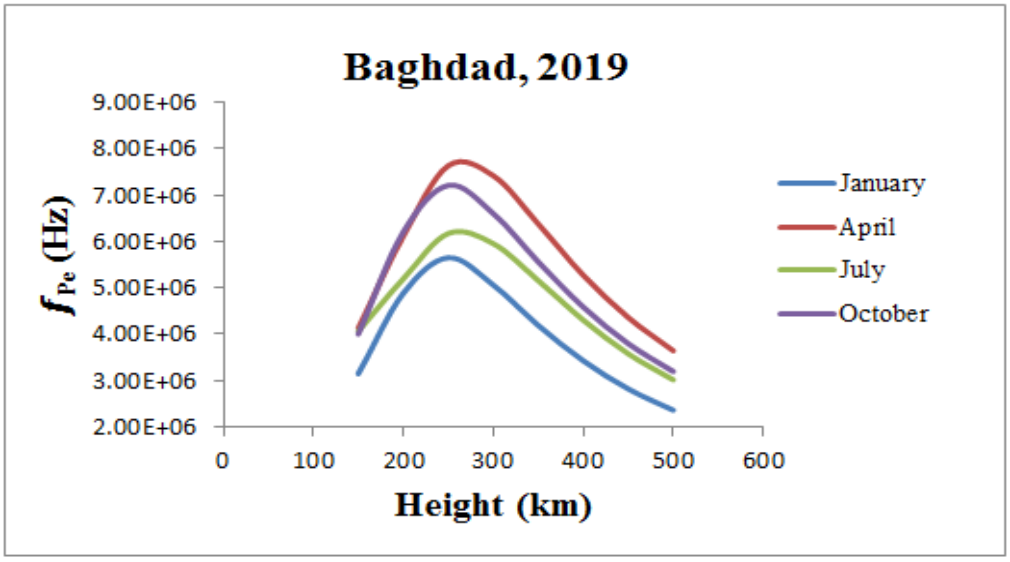

Figure 8-Represented the variation of Plasma frequency of electron, f_{Pe} (Hz) at 12 PM of F-ionosphere layer at different altitudes (150 − 500) km with 50 km increment in (January, April, July and October).

Figure-9 shows that seasonal variation for the number of charged particles (electrons and ions) N_D contained within a sphere of radius λ_D must be large and then $N_{De} \gg 1$, enough to achieve the collective behavior of plasmas.

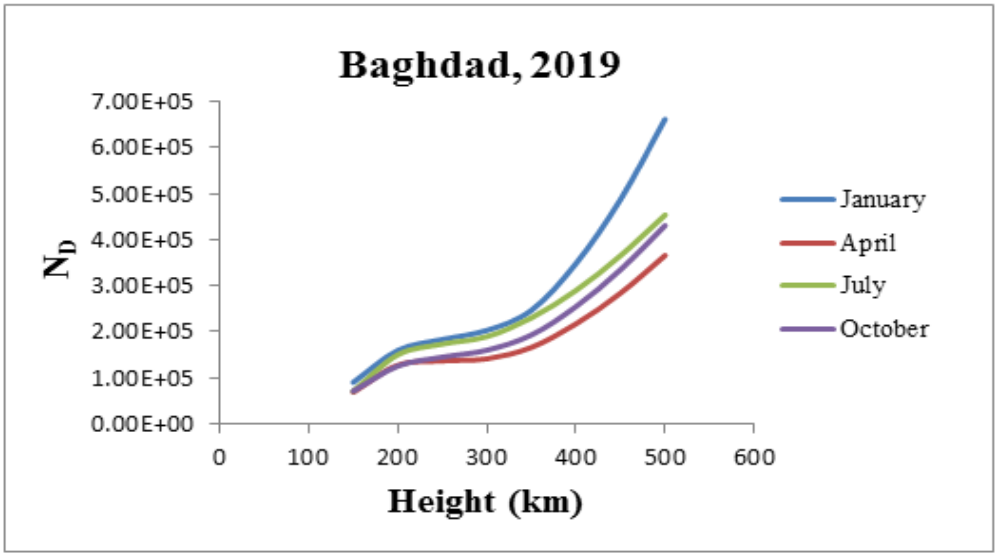

Figure 9-Represented the variation of Number of particles, N_D at 12 PM of F-ionosphere layer calculated at different altitudes (150 − 500) km with 50 km increment in (January, April, July and October).

Figure-10 shows at an altitude of 150 km, which is within the elevation range of the F1 layer, the seasonal variation for coupled plasma reached a maximum value due to the low rate of electron density for this height. While at higher altitudes it began to decline until it reached its lowest value. As a result of the high temperature of the electrons which led to the spread of particles in a Debye sphere, and due to this diffusion, the plasma became weakly coupled. In addition, coupled plasma around the equinoxes (April and October) were higher than those in summer or winter for solar minimum (2019) .This was due to a phenomenon called seasonal anomaly.

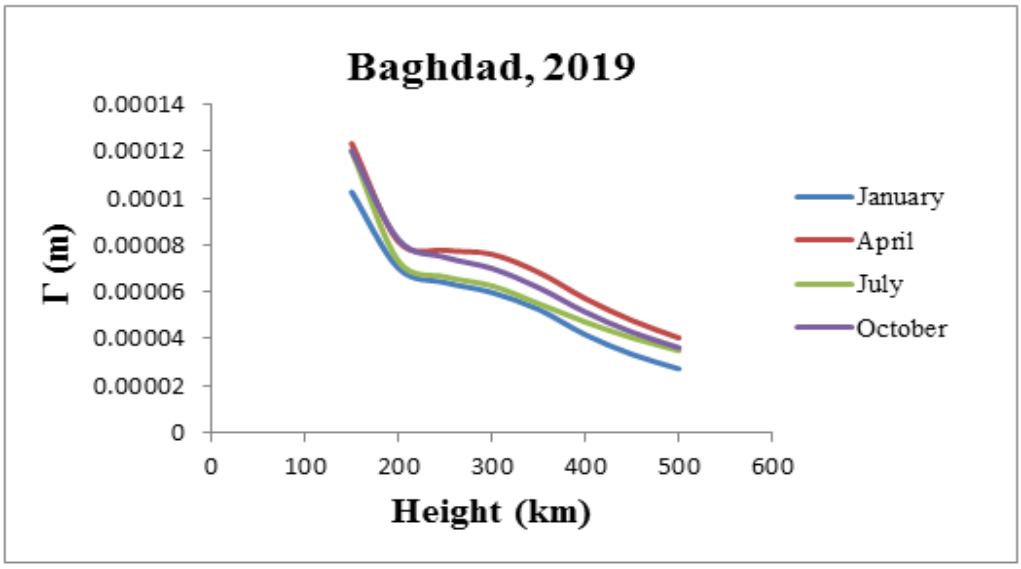

Figure 10-Represented the variation of Plasma coupling parameter of electron Γ (m) at 12 PM of F-ionosphere layer at different altitudes (150 − 500) km with 50 km increment in (January, April, July and October)

Figures-5 and -11 show the direct proportional between thermal velocity of electron and electron temperature. Thermal velocity of electron increased with altitudes due to the electron temperature which was increased with altitudes, as shown in figures 5.

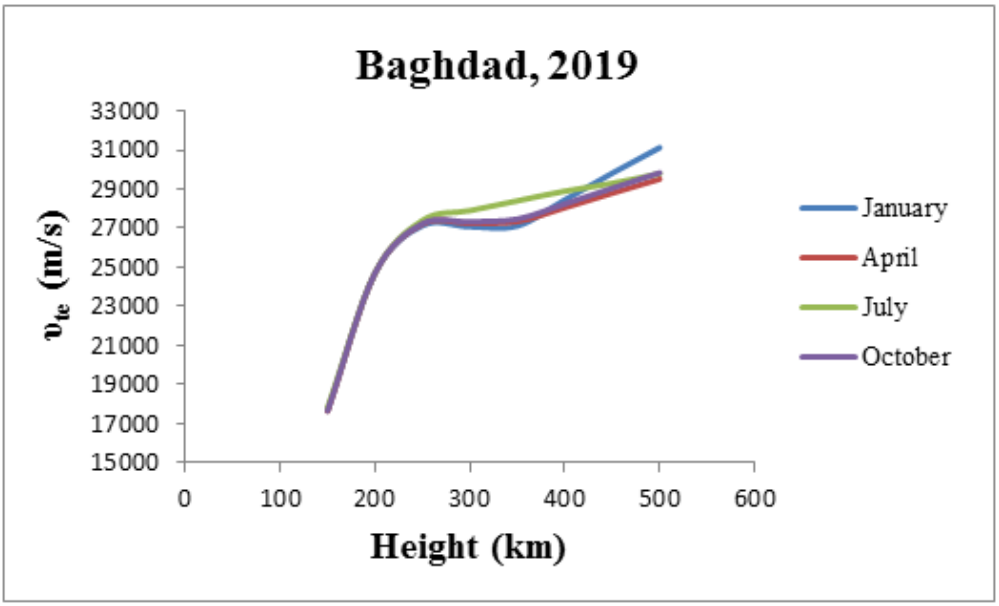

Figure 11-Represented the variation of Thermal velocity of electron, υ_{te} (m/s) at 12 PM of F-ionosphere layer at different altitudes (150 − 500) km with 50 km increment in (January, April, July and October).

5. Conclusions

This study has proved the plasma frequencies of electron, $\boldsymbol{f}_{Pe}$ and electron density, n_e around the equinoxes (April and October) were higher than those in summer and winter for solar minimum (2019). In general, it has been found that the seasonal variations behavior of the electron temperature (T_e) is similar at low altitudes (~200 km) in all months and its values increase by increasing the height. A positive correlation between υ_{te} and T_e was explained in all seasonal variations of ionosphere for the selected year. Additionally, λ_{De} around the equinoxes (April and October) was lower than that of summer or winter for solar minimum (2019). In this work, it has been proved that the electron coupling parameter in ionosphere is a weak ($\Gamma \ll 1$) in all seasons of the year (2019).

References

[1] P. Koucká Knížová, J. Laštovička, D. Kouba, Z. Mošna, K. Podolská and K. Potužníková, " Ionosphere influenced from lower-lying atmospheric regions," Frontiers in Astronomy and Space Sciences, vol. 8, p. 651445, 2021.

[2] O. Mingalev, G. Mingaleva, M. Melnik and V. S. Mingalev, "Numerical simulation of the time evolution of small-scale irregularities in the F-layer ionospheric plasma," International Journal of Geophysics,vol.2011, pp. 2-7, 2011,

[3] M. Sodha and S. Mishra, "Modification of electron density in F layer of ionosphere by dust suspension," Physics of Plasmas, vol. 24, no. 4, pp. 043705, 2017.

[4] W. S. Hussein, A. F. Ahmed and K.A. Aadim, "Influence of laser energy and annealing on structural and optical properties of CdSfilms prepared by laser induced plasma," Iraqi Journal of Science, vol. 61, no. 6, pp. 1307–1312, 2020.

[5] Q. A. Abbas, A. F. Ahmed , F.A-H. Mutlak, "Spectroscopic analysis of magnetized hollow cathode discharge plasma characteristics," Optik, vol.242, P.167260, 2021.

[6] A. A. Yousef, A. F. Ahmed, "Spectroscopic Analysis of DC-Nitrogen Plasma Produced using opper Electrodes," Iraqi Journal of Science, vol. 62, no. 10, pp. 3560-3569,2021.

[7] S.J. Schwartz, C.J. Owen, and D. Burgess, "Astrophysical plasmas," Astronomy Unit, Queen Mary, University of London, PP. 11- 45, 2004.
[8] S. Bora, "Ionosphere and radio communication," Resonance, vol. 22, pp. 123-133, 2017.
[9] Z. Wu, " A study of the F3 layer and ionospheric horizontal gradient observed by the arecibo incoherent scatter radar," Master's thesis, Miami University, 2017
[10] A. Anuar, "A study of dusty plasma environment," Lancaster University (United Kingdom), 2013, PP. 27-187.
[11] E. Engwall, "Cold magnetospheric plasma flows: Properties and interaction with spacecraft," Uppsala Univ., Sweden, vol. pp. 3- 34. 2006.
[12] R. O. Dendy, "Plasma dynamics," Oxford University Press, 1990, p. 176.
[13] F.F. Chen, " Introduction to plasma physics and controlled fusion," Springer, vol. 1, 1984.
14] L. Conde, "An introduction to plasma physics and its space applications," Department of Applied Physics ETS Ingenieros Aeronáuticos Universidad Politécnica de Madrid, 2014, pp. 6-22.
[15] A. Vértes , S. Nagy, Z. Klencsár, R. Lovas and F. Rösch, "Handbook of Nuclear Chemistry," Springer, vol. 4, pp. 1855- 2179, 2003.
[16] D. Bilitza, D. Altadill, V. Truhlik, V. Shubin, I. Galkin, B. Reinisch and X. Huang, "International Reference Ionosphere 2016: From ionospheric climate to real-time weather predictions" Space weather, vol. 15, pp. 418-429, 2017.
[17] D. Bilitza, "IRI the International Standard for the Ionosphere" Advances in Radio Science, vol. 16, pp.1- 11, 2018.
[18] The Sunspot Cycle, "Marshall Space Flight Center, "NASA, USA, November, 2018. Available: http://solarscience.msfc.nasa.gov/SunspotCycle.